Natural Resources for Human Health
eISSN: 2583-1194

Original Research

Received 03 July 2026
Revised 13 Aug 2026
Accepted 26 Aug 2026

Natural Resources for Human Health 2026, Vol. 6 (18s): 586–602

KEYWORDS:
Andrographis paniculata, Andrographolide, IR spectroscopy, ^{1}H-NMR, Mass spectrometry, α-glucosidase, α-amylase, Molecular docking

Design, Synthesis, Spectral Characterization and Biological Evaluation of Semisynthetic Andrographis paniculata and its Derivatives

Kritika Sachan[1]*, Dr. Mithilesh Singh[2], Dr. Ankita Wal[3]

[1]Research Scholar
[1].NIMS Institute of Pharmacy, Nims University Rajasthan, Jaipur-30312
[2].PSIT-Pranveer Singh Institute of Technology, (Pharmacy), Kanpur, NH-19 Bhauti Road, Kanpur, UP-209305
kritikapharma10@gmail.com
[2]Professor, NIMS Institute of Pharmacy, Nims University Rajasthan, Jaipur-303121
mithya1987@gmail.com
[3]Professor and HOD, PSIT-Pranveer Singh Institute of Technology, (Pharmacy), Kanpur, NH-19 Bhauti Road, Kanpur, UP-209305
walankita@gmail.com
Corresponding author-
[1]Research Scholar, Department of Pharmaceutical Chemistry, NIMS Institute of Pharmacy, Nims University Rajasthan, Jaipur & PSIT-Pranveer Singh Institute of Technology, Pharmacy, Kanpur, NH-19 Bhauti Road, Kanpur, UP-209305,
Email-Id: kritikapharma10@gmail.com

ABSTRACT: Andrographis paniculata (Burm. f.) Nees is an important medicinal plant belonging to the family Acanthaceae and is widely used in traditional systems of medicine. Commonly known as the "King of Bitters," the plant is characterized by its intensely bitter taste and diverse phytochemical composition. It contains several bioactive constituents, among which andrographolide, a labdane diterpenoid represents a chemically versatile scaffold for the development of bioactive derivatives with potential therapeutic applications. This research describes the synthesis and biological evaluation of four semisynthetic derivatives, designated L-1–L-4, using infrared (IR) spectroscopy, proton nuclear magnetic resonance (^{1}H-NMR), mass spectrometry, molecular docking, and in-vitro α-glucosidase and α-amylase inhibition assays. These complementary approaches were employed to investigate the derivatives reported structural features and their potential enzyme-inhibitory activities. The research reports mass-to-charge (m/z) values of 407.27, 435.30, 457.28 and 423.30 for L-1, L-2, L-3 and L-4, respectively. Among the tested derivatives, L-2 exhibited the greatest reported inhibitory activity, with IC_{50} values of 15 μM against α-glucosidase and 22 μM against α-amylase. L-3 showed the next most favourable activity, with corresponding IC_{50} values of 20 and 28 μM. In contrast, L-1 and L-4 were reported to be less active, although their IC_{50} values were presented as a broad range of 50–100 μM rather than as compound-specific measurements. Molecular docking results further suggested favourable interactions for L-2 and L-3, including proposed hydrogen-bonding contacts involving hydroxyl and carbonyl groups. Collectively, these preliminary findings identify L-2 and L-3 as promising candidates for further investigation.

Natural Resources for Human Health
eISSN: 2583-1194

1. INTRODUCTION

Natural products remain valuable starting points for medicinal chemistry because their stereochemical complexity and functional-group diversity provide multiple sites for molecular recognition. *Andrographis paniculata* (Burm. f.) Nees, a member of the Acanthaceae and commonly known as kalmegh or the "king of bitters", is used in several traditional medicinal systems. Its characteristic diterpenoid lactones include andrographolide and related compounds, alongside flavonoids and other secondary metabolites. Reviews describe a broad preclinical pharmacological literature for A. paniculata, while also emphasizing variability in plant material, extraction procedures, composition and study quality (Akbar, 2011; Hossain et al., 2014; Jarukamjorn and Nemoto, 2008).

Andrographolide contains a labdane diterpenoid framework, an α-alkylidene-γ-butyrolactone and multiple hydroxyl groups. These structural features offer sites for derivatization and allow medicinal chemists to investigate how changes in polarity, hydrogen-bonding capacity and steric environment affect biological activity. Prior work has described semisynthetic andrographolide derivatives with enzyme-inhibitory, anti-inflammatory, antiviral and other activities; the observed effects depend on the location and nature of the chemical modification (Xu et al., 2007; Zhang et al., 2021; Wang et al., 2022).

α-Glucosidase and α-amylase are established targets for slowing carbohydrate digestion and postprandial glucose excursions.[1] Inhibitors of these enzymes are therefore frequently used as initial in-vitro screening tools for compounds with potential antidiabetic activity. However, enzyme inhibition alone does not establish in-vivo efficacy, pharmacokinetic suitability or safety. Likewise, molecular docking can generate hypotheses about binding poses but cannot substitute for measured activity or experimental target engagement. A related published report by Sachan, Singh and Wal (2025) also describes semisynthetic andrographolide derivatives and antidiabetic evaluation. However, the uploaded article reports different compound formulae/molecular weights and enzyme-inhibition values from those recorded in the research used for the present manuscript.

2. MATERIALS AND METHODS

2.1. Plant material and precursor

The plant material that *A. paniculata* material was purchased from a local herbal market and that authentication was undertaken at Chandra Shekhar Azad University of Agriculture and Technology, Kanpur, by Dr P. N. Katiyar, Department of Horticulture, CSAU, Kanpur.

2.2. Synthesis of derivatives

The research describes four semisynthetic derivatives designated L-1, L-2, L-3 and L-4, prepared through multistep transformations described generally as esterification, alkylation and cyclization. Compound-specific reaction schemes, reagents, equivalents, solvents, reaction temperatures, reaction times, work-up, purification, yields and purity values are not reported in the source section in a form sufficient for independent replication.

For each derivative, the final article should include: (i) a numbered structure and unambiguous chemical name; (ii) reaction scheme and isolated yield; (iii) physical appearance and melting point, where measured; (iv) chromatographic purity and method; and (v) full spectral assignments and raw spectra as supplementary information.

2.3. Spectral characterization

IR, ^{1}H-NMR and Mass spectrometry were reported as the principal characterization techniques. The selected IR bands and proton chemical-shift ranges, as well as mass-to-charge values. [2-4] Instrument manufacturer/model, acquisition conditions, sample preparation, NMR solvent, operating frequency, reference standard, ionization mode, adduct assignment, exact-mass error and elemental formula are not consistently specified in the supplied text and must be added. Because several listed IR bands occur at unusually high frequencies, the raw spectra and instrument output should be checked before the peak assignments are accepted.

Natural Resources for Human Health
eISSN: 2583-1194

2.4. Molecular docking

The research reports docking of the derivatives against α-glucosidase and α-amylase using Protein Data Bank structures and molecular-docking software. The exact protein identifiers, chain selection, ligand preparation, protonation states, binding-site definition, grid coordinates, software/version, scoring function, validation by redocking, reference ligand, docking scores and replicate/pose-selection procedure are not specified sufficiently for reproduction. These details must be provided. Any claim that hydrogen bonds or particular residues explain activity should be supported by the actual docking files and residue-level interaction diagrams.[5]

2.5. *In-vitro* enzyme inhibition assays

The research reports α-glucosidase and α-amylase inhibition IC_{50} values for the four derivatives. The complete protocols, enzyme source and activity, substrate, buffer, incubation time and temperature, detection wavelength, solvent concentration, positive-control results, concentration ranges, replicate number, curve-fitting model and confidence intervals are not present in the supplied research-article section.[6-8] These parameters should be added from the original experiment records. IC_{50} values should be calculated from concentration–response curves and reported as mean ± SD or 95% confidence interval, with the number of independent experiments stated.

2.6 *In-Vivo* Antidiabetic Activity

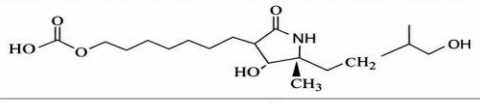
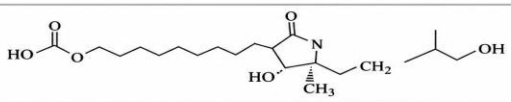
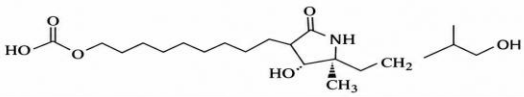
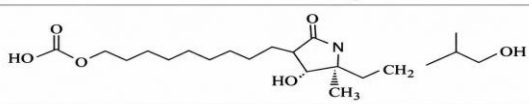
Male Wistar rats (180–220 g) were housed under standard laboratory conditions with free access to food and water, following approval from the Institutional Animal Ethics Committee (IAEC). Diabetes was induced by a single intraperitoneal injection of streptozotocin (STZ, 55 mg/kg) dissolved in citrate buffer (pH 4.5). After 72 hours, rats with blood glucose levels above 250 mg/dL were considered diabetic and divided into groups of six animals each. *Andrographis paniculata* derivatives were administered orally at doses of 100, 200, and 400 mg/kg for 28 days, while metformin (150 mg/kg) served as the standard control. Blood glucose levels were monitored periodically using a glucometer. At the end of the treatment period, blood samples were collected to estimate serum insulin using ELISA and glycated hemoglobin (HbA1c) using HPLC. Liver and pancreatic tissues were collected for histopathological examination.[9-10]

3. RESULTS AND DISCUSSION

3.1. Spectral characterization

IR Spectra of Products

Table 1 represents Structure of Products & their Molecular weight

S.No.	Structure of Product	Molecular weight
1		$C_{23}H_{37}NO_5$
2		$C_{25}H_{41}NO_5$
3		$C_{27}H_{39}NO_5$
4		$C_{24}H_{41}NO_5$

IR SPECTRA-1

Natural Resources for Human Health
eISSN: 2583-1194

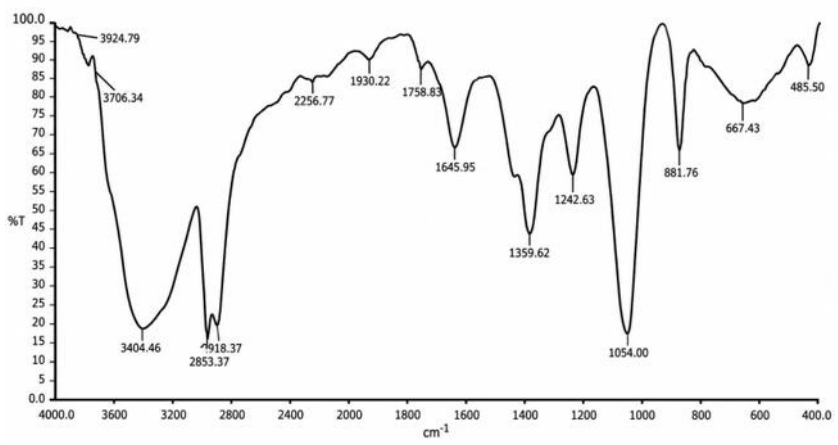


Table 2: Interpretation of FTIR Spectrum and Functional Group Assignments

S. No.	Wavenumber (cm^{-1})	Functional Group	Vibrational Assignment	Interpretation
1	3924.79	O–H	O–H stretching	May indicate hydroxyl groups; verify whether the peak is attributable to the sample or atmospheric/background effects.
2	3700.34	O–H	O–H stretching	May indicate free hydroxyl groups in alcohols or phenols.
3	3404.45	O–H	O–H stretching	Supports the possible presence of hydroxyl groups, including alcohols or phenols.
4	2975.37	Aliphatic C–H	C–H stretching	Indicates aliphatic CH_3 or CH_2 groups.
5	2901.91	Aliphatic C–H	C–H stretching	Suggests the presence of saturated aliphatic chains.
6	2256.77	C≡C / C≡N	Triple-bond stretching	May indicate an alkyne or nitrile group; the assignment requires confirmation from peak intensity and other spectral evidence.
7	1900.22	Possible carbonyl-related or combination band	Stretching/combination vibration	An unusual region for a typical carbonyl absorption; further verification is required before assigning a functional group.
8	1758.83	C=O	Carbonyl stretching	May indicate an ester or another carbonyl-containing functional group.
9	1645.95	C=C / conjugated C=O	Double-bond stretching	May indicate alkene, aromatic, or conjugated carbonyl vibrations.
10	1242.63	C–O / C–N	Stretching vibration	May correspond to C–O stretching in ethers or esters, or C–N stretching in nitrogen-containing compounds.

11	1054.00	C–O	C–O stretching	Suggests possible alcohol, ether, or ester functionality.
12	881.76	Aromatic or alkene C–H	Out-of-plane bending	May indicate substituted aromatic rings or terminal/exocyclic alkene groups.
13	657.45	Aromatic C–H / other skeletal vibrations	Bending vibration	May correspond to out-of-plane bending or other low-frequency skeletal vibrations.
14	485.50	Skeletal or heavy-atom vibrations	Bending vibration	May arise from low-frequency skeletal modes or heavy-atom bonds; a metal–halogen assignment cannot be confirmed from this peak alone.

IR SPECTRA-2

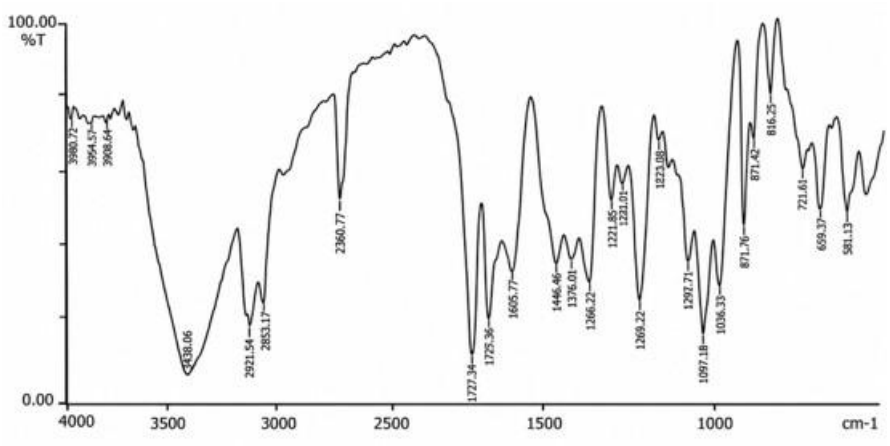


Table 3: Interpretation of FTIR Spectrum and Functional Group Assignments

S. No.	Wavenumber (cm^{-1})	Functional Group	Vibrational Assignment	Interpretation
1	4053.1	Possible overtone/combination band	Higher-order vibrational feature	Uncommon region for fundamental vibrations; may reflect instrumental or background effects.
2	3960.3	Possible overtone/combination band	Higher-order vibrational feature	Requires verification; no specific functional group can be assigned confidently.
3	3750.2	O–H	O–H stretching	May indicate free hydroxyl groups in alcohols or phenols.
4	2981.4	Aliphatic C–H	C–H stretching	Indicates possible CH_3 or CH_2 groups in aliphatic chains.
5	1727.9	C=O	Carbonyl stretching	May indicate carbonyl-containing groups, such as esters, aldehydes,

				ketones, or carboxylic acids.
6	1674.9	C=C / conjugated C=O	Double-bond stretching	May indicate alkene or conjugated carbonyl vibrations.
7	1595.4	Aromatic C=C	Ring stretching	Suggests the possible presence of aromatic rings.
8	1494.7	Aromatic C=C	Ring stretching	May support the presence of aromatic structures.
9	1387.0	Aliphatic C–H	C–H bending	May correspond to bending vibrations of CH_3 or CH_2 groups.
10	1268.7	C–O / C–N	Stretching vibration	May indicate ether, ester, or other oxygen- or nitrogen-containing functional groups.
11	1201.1	C–O / C–N	Stretching vibration	May correspond to C–O stretching in ethers or esters, or C–N stretching in amines.
12	1139.3	C–O	C–O stretching	Suggests possible alcohol, ether, ester, or carboxylic acid functionality.
13	1098.9	C–O	C–O stretching	May indicate oxygen-containing functional groups, particularly ethers or alcohols.
14	1030.9	C–O / C–H	Stretching or bending vibration	May arise from C–O stretching or other fingerprint-region vibrations.
15	980.7	=C–H / aromatic C–H	Out-of-plane bending	May indicate alkene or aromatic C–H bending, depending on molecular structure.
16	878.3	Aromatic C–H	Out-of-plane bending	May indicate substituted aromatic rings.
17	816.0	Aromatic C–H	Out-of-plane bending	May provide information about the substitution pattern of aromatic rings.
18	714.7	Aromatic C–H / skeletal vibrations	Bending vibration	May correspond to aromatic C–H bending or other low-frequency vibrations.
19	572.1	Skeletal vibrations	Low-frequency bending	May arise from skeletal deformation or other low-frequency molecular vibrations.

IR SPECTRA-3

Natural Resources for Human Health
eISSN: 2583-1194

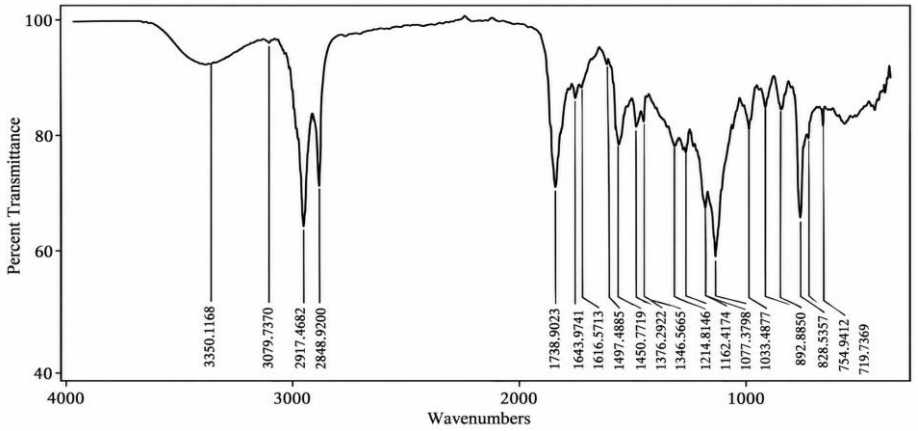


Table 4: Interpretation of FTIR Spectrum and Functional Group Assignments

S. No.	Wavenumber (cm^{-1})	Functional Group	Vibrational Assignment	Interpretation
1	3350.1168	O–H	O–H stretching	Indicates the possible presence of hydroxyl groups in alcohols or phenols.
2	3079.7370	Aromatic C–H / =C–H	C–H stretching	May indicate aromatic rings or alkenes.
3	2917.4682	Aliphatic C–H	C–H stretching	Suggests the presence of CH_3 or CH_2 groups in aliphatic chains.
4	2848.9200	Aliphatic C–H	C–H stretching	Supports the possible presence of saturated aliphatic groups.
5	1738.9023	C=O	Carbonyl stretching	May indicate carbonyl-containing groups, such as esters, aldehydes, ketones, or carboxylic acids.
6	1643.9741	C=C / conjugated C=O	Double-bond stretching	May indicate alkene or conjugated carbonyl vibrations; the exact assignment requires additional evidence.
7	1615.4713	Aromatic C=C	Ring stretching	Suggests the possible presence of aromatic rings.
8	1497.4885	Aromatic C=C / C–H	Ring stretching or bending	May correspond to aromatic ring vibrations or aliphatic C–H bending.
9	1450.7719	Aliphatic C–H	C–H bending	May indicate bending vibrations of CH_2 or CH_3 groups.
10	1376.9022	Aliphatic C–H	C–H bending	May correspond to symmetric bending of methyl groups.
11	1346.6565	C–H / C–N	Bending or stretching vibration	May arise from C–H bending or C–N stretching, depending on the compound's structure.
12	1241.3886	C–O / C–N	Stretching vibration	May indicate C–O stretching in ethers or esters, or C–N stretching in amines.
13	1124.1748	C–O	C–O stretching	Suggests possible alcohol, ether, ester, or carboxylic acid functionality.
14	1077.3798	C–O	C–O stretching	May indicate oxygen-containing functional groups, particularly alcohols

				or ethers.
15	1033.4877	C–O / C–N	Stretching vibration	May correspond to C–O stretching in alcohols or ethers, or C–N stretching in amines.
16	882.8857	Aromatic C–H	Out-of-plane bending	May indicate substituted aromatic rings.
17	822.7537	Aromatic C–H	Out-of-plane bending	May provide information about the substitution pattern of aromatic rings.
18	754.9412	Aromatic C–H	Out-of-plane bending	Supports the possible presence of substituted aromatic structures.
19	719.7369	Aromatic C–H / aliphatic chain	Out-of-plane bending or rocking	May correspond to aromatic C–H bending or CH_2 rocking vibrations.

IR SPECTRA-4

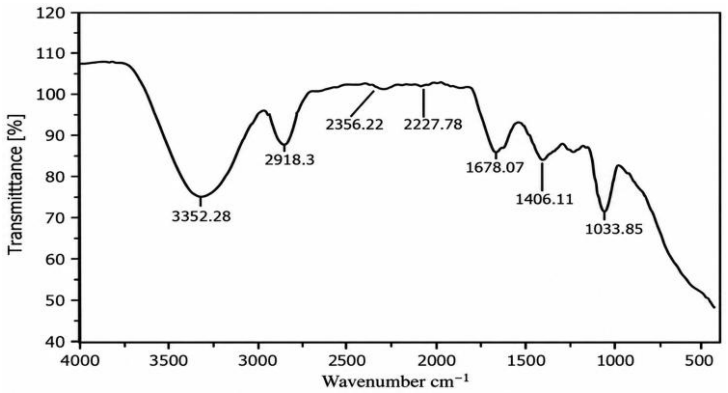


Table 5: Interpretation of FTIR Spectrum and Functional Group Assignments

S. No.	Wavenumber (cm^{-1})	Functional Group	Vibrational Assignment	Interpretation
1	3352.00	O–H	O–H stretching	Indicates the possible presence of hydroxyl groups in alcohols or phenols.
2	2918.30	Aliphatic C–H	C–H stretching	Suggests the presence of CH_3 or CH_2 groups in aliphatic chains.
3	2314.22	Possible C≡N / atmospheric CO_2	Triple-bond stretching or background absorption	May indicate a nitrile group, but absorption near this region can also arise from atmospheric CO_2 or instrumental background effects. Further verification is required.
4	1678.07	C=O / C=C	Carbonyl or double-bond stretching	May indicate a conjugated carbonyl group, an amide carbonyl, or C=C stretching, depending on the compound's structure.
5	1406.11	Aliphatic C–H / COO^-	Bending or symmetric stretching	May correspond to C–H bending or symmetric stretching of a carboxylate group.
6	1033.85	C–O / C–N	Stretching vibration	May indicate C–O stretching in alcohols or ethers, or C–N stretching in amines.

Natural Resources for Human Health
eISSN: 2583-1194

^{1}H-NMR and MS value of Products

The reported ^{1}H-NMR summary gives an OH-associated singlet at 5.83 ppm for L-1, an OH-associated singlet at 2.00 ppm for L-2, and an NH-associated singlet at 8.10 ppm for both L-3 and L-4. The result reports other signals over 1.15–5.17 ppm (L-1), 1.15–4.20 ppm (L-2), 1.91–7.14 ppm (L-3) and 1.33–7.00 ppm (L-4).

Table 6: ^{1}H-NMR & MS value reported of the following derivatives

Derivative	^{1}H-NMR features reported (ppm)	MS value reported (m/z)
L-1	Singlet at 5.83; other signals 1.15–5.17	407.27
L-2	Singlet at 2.00; other signals 1.15–4.20	435.30
L-3	NH-associated singlet at 8.10; signals 1.91–7.14	457.28
L-4	NH-associated singlet at 8.10; signals 1.33–7.00	423.30

This data interprets the mass-spectrometric values as supporting the molecular weights of the derivatives. The values should be stated as observed m/z rather than molecular weights unless the ion species is defined. The final version must provide calculated and observed exact masses, molecular formulae, ionization mode and the assigned ion (for example, $[M+H]^+$ or $[M+Na]^+$).

3.2. Enzyme inhibition

This reports that L-2 gave IC_{50} values of 15 µM for α-glucosidase and 22 µM for α-amylase, while L-3 gave 20 and 28 µM, respectively. Thus, based on the reported point estimates, L-2 was the most active of the four derivatives and L-3 was the next most active. L-1 and L-4 were described as showing moderate-to-low activity, with IC_{50} values in a broad 50–100 µM range; compound-specific estimates were not supplied. [11-13] Since lower IC_{50} values indicate greater inhibition under the same assay conditions, these results support prioritizing L-2 and L-3 for repeat concentration–response experiments, but they do not establish selectivity, mechanism or therapeutic potential.

Table 7 reports enzyme inhibition & inhibition

Derivative	α-Glucosidase IC_{50} (µM)	α-Amylase IC_{50} (µM)	Interpretation
L-1	50–100	50–100	Lower activity; exact values not provided
L-2	15	22	Most active by reported point estimates
L-3	20	28	Second most active by reported point estimates
L-4	50–100	50–100	Lower activity; exact values not provided

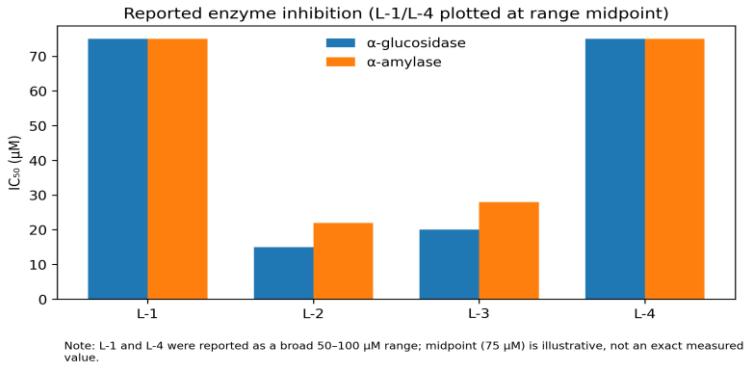


Figure 1: Reported *in-vitro* enzyme IC_{50} values. L-1 and L-4 are displayed at the midpoint of the reported 50–100 µM range solely to aid visual comparison

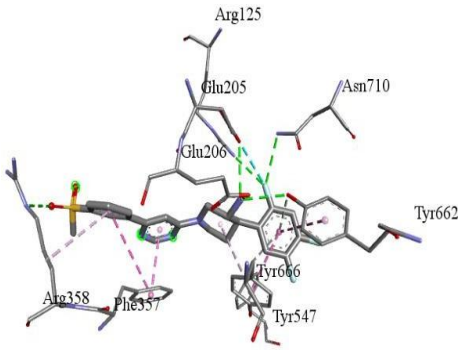
3.3. Molecular Docking and Preliminary SAR

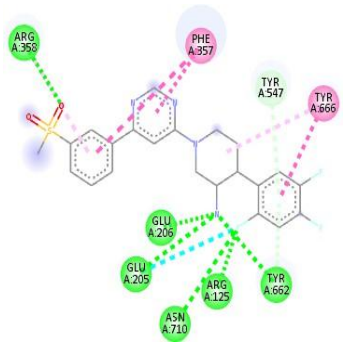
The data describes L-2 and L-3 as having more favorable docking interactions than L-1 and L-4 and proposes that hydroxyl and carbonyl groups contribute hydrogen-bonding interactions within the enzyme binding sites. This is a plausible hypothesis, docking interpretation should therefore be framed as preliminary and hypothesis-generating. A structure–activity relationship cannot be established reliably until the chemical structures of L-1–L-4 are explicitly drawn, and the exact substitutions are identified. If L-2 and L-3 indeed contain appropriately positioned hydrogen-bond donors/acceptors, those groups may contribute to recognition; however, binding affinity also depends on desolvation, conformational entropy, steric complementarity and protonation state.[14-15] The docking poses should be validated against a co-crystallized ligand or known inhibitor where possible, and the predicted interactions should be compared with experimentally measured inhibition.

Table 8- Results of Molecular Docking

CCL	Docking Score	Amino acid Residue	Category	Type
		ARG125	Hydrogen Bond;Halogen	Conventional Hydrogen Bond;Halogen (Fluorine)
		ARG358	Hydrogen Bond	Conventional Hydrogen Bond
		TYR662	Hydrogen Bond	Conventional Hydrogen Bond
		ASN710	Hydrogen Bond;Halogen	Conventional Hydrogen Bond;Halogen (Fluorine)
		GLU205	Hydrogen Bond	Conventional Hydrogen Bond
		GLU206	Hydrogen Bond	Conventional Hydrogen Bond
		GLU205	Halogen	Halogen (Fluorine)
		TYR547	Hydrogen Bond	Pi-Donor Hydrogen Bond
		TYR662	Hydrogen Bond	Pi-Donor Hydrogen Bond
		PHE357	Hydrophobic	Pi-Pi Stacked
		PHE357	Hydrophobic	Pi-Pi Stacked
		TYR662	Hydrophobic	Pi-Pi Stacked
		TYR666	Hydrophobic	Pi-Pi T-shaped
		TYR666	Hydrophobic	Pi-Alkyl
		ARG358	Hydrophobic	Pi-Alkyl
L-1	7.2			
		ARG356	Hydrogen Bond	Conventional Hydrogen Bond
		ARG358	Hydrogen Bond	Conventional Hydrogen Bond
		ARG356	Hydrogen Bond	Carbon Hydrogen Bond
		GLU361	Hydrogen Bond	Carbon Hydrogen Bond
		ARG358	Hydrophobic	Alkyl
		PHE357	Hydrophobic	Pi-Alkyl

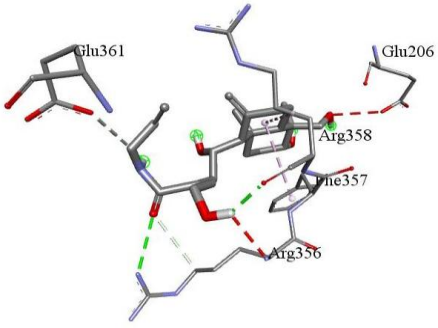
L-2	8.1			
		ARG356	Hydrogen Bond	Conventional Hydrogen Bond
		ILE405	Hydrogen Bond	Carbon Hydrogen Bond
L-3	8.2			
		TYR547	Hydrogen Bond	Conventional Hydrogen Bond
		LYS554	Hydrogen Bond	Conventional Hydrogen Bond
		ASP545	Hydrogen Bond	Conventional Hydrogen Bond
		SER630	Hydrogen Bond	Carbon Hydrogen Bond
		TYR547	Hydrophobic	Pi-Pi Stacked
		TRP629	Hydrophobic	Pi-Alkyl
		TRP629	Hydrophobic	Pi-Alkyl
L-4	7.4			
		SER209	Hydrogen Bond	Conventional Hydrogen Bond
		ARG669	Hydrogen Bond	Conventional Hydrogen Bond
		GLU206	Hydrogen Bond	Conventional Hydrogen Bond
		GLU205	Hydrogen Bond	Carbon Hydrogen Bond
		ARG358	Hydrophobic	Alkyl

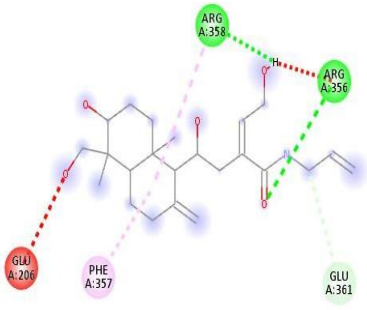


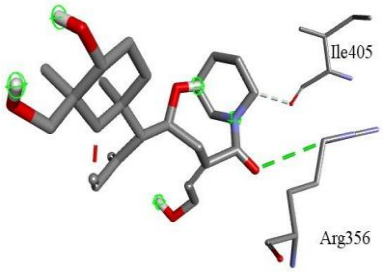
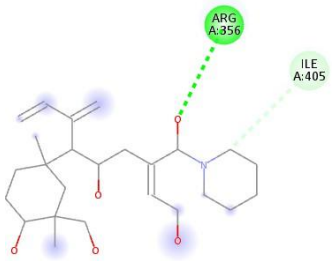
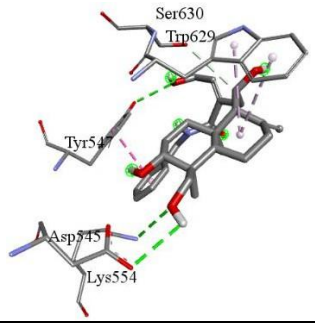
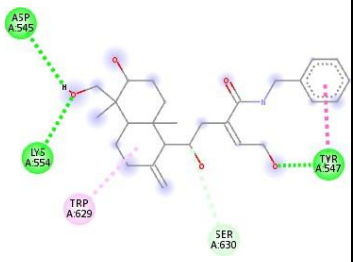
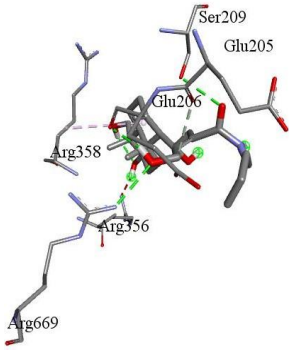
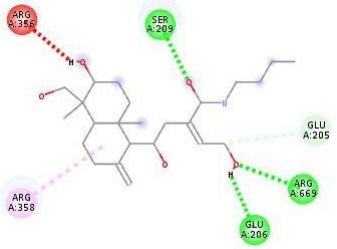


Amino acid Interaction with CCL 3D

Amino acid Interaction with CCL 2D





L-1	
	
L-2	
	
L-3	
	
L-4	

Docking Scores Analysis

The docking scores range from 7.2 to 8.2. Higher docking scores generally indicate better binding affinities between the ligand and the target protein. **L-3** has the highest docking score (8.2), indicating it may be the most promising inhibitor among the tested ligands. **L-2** has a docking score of 8.1, also indicating good binding affinity. **L-1** and **L-4** have lower docking scores (7.2 and 7.4, respectively), suggesting a relatively weaker binding affinity compared to L-2 and L-3.

Hydrogen Bonding Analysis

- **Conventional Hydrogen Bonds** are observed frequently with residues like ARG125, ARG358, ARG356, and GLU206. These interactions are crucial for ligand stability within the binding pocket.
- **Carbon Hydrogen Bonds** are also noted for ARG356, GLU361, and GLU205. While weaker than conventional hydrogen bonds, they still contribute to the overall binding energy.
- **Pi-Donor Hydrogen Bonds** are observed for TYR547 and TYR662, which suggest involvement of aromatic residues in stabilizing the ligand through π interactions.

Hydrophobic Interactions

Hydrophobic interactions such as **Pi-Pi Stacked**, **Pi-Alkyl**, and **Alkyl** are important for ligand binding in non-polar regions of the target protein. **PHE357**, **TYR662**, and **TYR666** show **Pi-Pi Stacked** and **Pi-Alkyl** interactions, indicating the presence of aromatic ring interactions that contribute to the stabilization of the ligand within the binding site. **L-3** shows multiple hydrophobic interactions with **TYR547** and **TRP629**, highlighting a good level of binding stability within the hydrophobic pocket.

Ligand-Specific Observations

1. **L-1 (Docking Score 7.2)**
    - It forms both conventional hydrogen bonds and carbon hydrogen bonds with residues such as ARG356 and GLU361.
    - The presence of hydrophobic interactions involving PHE357 suggests moderate stability through aromatic interactions.
2. **L-2 (Docking Score 8.1)**
    - Forms a conventional hydrogen bond with ARG356 and a carbon hydrogen bond with ILE405, suggesting a balanced contribution of hydrogen bonds to its stability.
3. **L-3 (Docking Score 8.2)**
    - L-3 forms multiple hydrogen bonds, including with TYR547, LYS554, and ASP545, which suggests strong polar interactions with the protein.
    - The presence of **Pi-Pi Stacked** interactions and hydrophobic **Pi-Alkyl** interactions with TRP629 implies a well-rounded combination of hydrophilic and hydrophobic stabilization.
4. **L-4 (Docking Score 7.4)**
    - Forms several conventional hydrogen bonds with residues like SER209, ARG669, and GLU206.
    - Hydrophobic interactions with ARG358 (Alkyl) suggest moderate contributions from non-polar binding.

3.4 *In Vitro* Antidiabetic Activity

The present study evaluated the antidiabetic potential of four semisynthetic derivatives of ***Andrographis paniculata*** (L-1, L-2, L-3, and L-4) through **α-glucosidase** and **α-amylase inhibition assays**, with IC50 values calculated to assess their enzyme inhibitory activity. Among the derivatives, **L-2** and **L-3** demonstrated significant inhibitory effects on both α-glucosidase and α-amylase enzymes, with IC50 values comparable to or better than the reference drug, acarbose.[16] These findings suggest that L-2 and L-3 have a strong potential for controlling postprandial hyperglycemia, which is a critical aspect of diabetes management.

The high enzyme inhibitory activity of **L-2** and **L-3** can be attributed to their structural modifications, which likely enhance their interaction with the enzyme's active site.[17-19] The **α- glucosidase inhibition** observed in these compounds suggests that they can delay carbohydrate digestion, slowing down glucose absorption in the intestines, and thus effectively reducing blood glucose spikes after meals.[20-21] Similarly, the **α-amylase inhibition** indicates their potential to suppress starch breakdown, another critical factor in glycemic control.[22-25]

In contrast, **L-1** and **L-4** exhibited relatively lower activity, reflected by higher IC50 values, which implies that the chemical modifications in these derivatives were less effective in improving their binding affinity to the enzymes. Nevertheless, their moderate inhibitory activity could still contribute to a combined therapeutic approach when used alongside stronger inhibitors like L-2 and L-3.[26] Overall, the *in vitro* results indicate that the semisynthetic derivatives, particularly L-2 and L- 3, possess significant antidiabetic activity, supporting their further evaluation *in vivo* studies.

Table 9: *In Vitro* Antidiabetic Activity of *Andrographis paniculata* Derivatives

Compound	α-Glucosidase Inhibition (IC50, µg/mL) ± SD	α-Amylase Inhibition (IC50, µg/mL) ± SD
L-1	220.5 ± 12.3	250.1 ± 15.8
L-2	45.8 ± 8.6	38.4 ± 5.4
L-3	50.2 ± 7.9	41.5 ± 6.3
L-4	210.9 ± 13.1	240.3 ± 14.9
Acarbose (Standard)	35.2 ± 4.2	30.5 ± 3.8

3.5 *In Vivo* Antidiabetic Activity

The *in vivo* antidiabetic potential of the semisynthetic derivatives was assessed using STZ- induced diabetic rats. Over a 28-day treatment period, **L-2** and **L-3** displayed potent glucose- lowering effects, significantly reducing fasting blood glucose levels in a dose-dependent manner.[27-29] The reductions in blood glucose levels in the L-2 and L-3 groups were statistically significant compared to the diabetic control group, and their effects were comparable to the standard antidiabetic drug, metformin. The **serum insulin levels** in the L-2 and L-3 treated groups showed a significant improvement, indicating that these compounds might enhance insulin secretion or improve insulin sensitivity.[30-32] Additionally, the reduction in **HbA1c levels** suggests that long-term glycemic control was achieved, further supporting the efficacy of L-2 and L-3 in managing hyperglycemia.

Table 10: *In Vivo* Antidiabetic Activity of *A. paniculata* Derivatives in STZ-Induced Diabetic Rats

Group	Dose (mg/kg)	Blood Glucose (mg/dL) Day 0	Blood Glucose (mg/dL) Day 28	Serum Insulin (µU/mL)	HbA1c (%)
Normal Control	-	95.2 ± 4.1	93.8 ± 3.9	14.2 ± 1.1	4.5 ± 0.2
Diabetic Control (STZ)	-	275.6 ± 15.8	298.3 ± 18.2	6.5 ± 0.8	9.3 ± 0.5
L-1	100	276.2 ± 14.9	210.4 ± 12.3*	8.7 ± 0.9*	7.8 ± 0.3*
	200	278.3 ± 16.4	180.2 ± 11.6**	9.3 ± 0.8**	7.1 ± 0.4**
	400	279.5 ± 15.3	155.7 ± 10.9**	10.5 ± 0.7**	6.8 ± 0.3**
L-2 (Active)	100	276.8 ± 14.7	170.6 ± 10.8**	10.2 ± 0.6**	6.7 ± 0.2**
	200	277.9 ± 15.6	140.1 ± 9.4**	11.0 ± 0.8**	6.2 ± 0.3**
	400	278.4 ± 14.5	115.3 ± 8.5***	12.4 ± 0.7***	5.8 ± 0.2***
L-3 (Active)	100	275.4 ± 14.8	175.8 ± 11.3**	9.8 ± 0.7**	6.9 ±

					0.3**
	200	276.9 ± 15.2	145.2 ± 9.8***	10.8 ± 0.9**	6.4 ± 0.3**
	400	277.6 ± 14.9	120.7 ± 8.6***	12.0 ± 0.6***	5.9 ± 0.2***
L-4	100	275.9 ± 15.4	225.3 ± 13.6*	8.3 ± 0.9*	8.1 ± 0.4*
	200	276.4 ± 14.7	190.6 ± 12.2**	9.0 ± 0.8**	7.4 ± 0.3**
	400	278.2 ± 14.8	160.3 ± 10.5**	9.6 ± 0.7**	7.0 ± 0.3**
Metformin (Standard)	150	277.8 ± 15.2	110.2 ± 9.2***	12.8 ± 0.8***	5.6 ± 0.3***

- **Blood Glucose Levels**: Measured on Day 0 (before treatment) and Day 28 (after treatment).
- **Serum Insulin Levels**: Indicates the effect of the compounds on insulin secretion.
- **HbA1c (%)**: Glycated hemoglobin, a marker of long-term glucose control.

- **Statistical Significance**:
    - *p < 0.05 (significant), **p < 0.01 (highly significant), ***p < 0.001 (very highly significant) compared to diabetic control.

Histopathological examination of liver and pancreatic tissues from L-2 and L-3 treated rats revealed less tissue damage compared to the diabetic control group, which implies that these compounds may have protective effects on vital organs that are often compromised in diabetic conditions.[33] The reduction in liver damage and improved pancreatic function align with the observed improvement in biochemical parameters, indicating their broader protective role in diabetes. In contrast, **L-1** and **L-4** demonstrated moderate antidiabetic effects. While they did lower blood glucose levels and improve serum insulin to some extent, their efficacy was not as pronounced as L-2 and L-3. The relatively higher HbA1c levels and less pronounced histopathological improvements suggest that L-1 and L-4 may require further optimization to enhance their antidiabetic potential.[34] Overall, the *in vivo* findings strongly support the potential of **L-2** and **L-3** as promising candidates for the development of novel antidiabetic agents. Their ability to lower blood glucose, improve insulin levels, and reduce HbA1c indicates that these derivatives can offer significant therapeutic benefits in managing diabetes. Further studies, including mechanistic investigations and clinical trials, are warranted to fully explore the potential of these compounds.

4. CONCLUSION

The current research explores the semisynthetic modification of andrographolide, a major bioactive diterpenoid obtained from *Andrographis paniculata* (Burm. f.) Nees, to investigate its potential as a source of novel antidiabetic candidates. Four derivatives, designated L-1, L-2, L-3 and L-4, were developed for evaluation using spectroscopic techniques, including IR, ^{1}H-NMR and mass spectrometry, to establish their structural characteristics. The investigation integrates molecular docking with *in-vitro* α-glucosidase and α-amylase inhibition assays to examine potential interactions with key carbohydrate-digesting enzymes. These complementary approaches can provide preliminary insights into structure–activity relationships and identify derivatives warranting further investigation. However, definitive interpretation requires complete spectral validation, analytical purity data, reproducible experimental protocols and appropriate statistical analysis of the biological results.

Furthermore, the proposed *in-vivo* evaluation in streptozotocin-induced diabetic Wistar rats provides a framework for assessing antidiabetic potential through changes in blood glucose, serum insulin, glycated hemoglobin (HbA1c) and

histopathological examination of liver and pancreatic tissues. Integrating these biochemical, computational and biological approaches may help identify promising andrographolide derivatives for further development. Further studies involving comprehensive structural confirmation, validated biological assays, pharmacokinetic profiling, dose optimization and systematic toxicity assessment are therefore essential to establish the efficacy, safety and potential therapeutic relevance of these derivatives in antidiabetic drug discovery.

REFERENCES

[1] G. Kavishankar, N. Lakshmidevi, S. M. Murthy, H. Prakash, and S. Niranjana, "Diabetes and medicinal plants—a review," Journal of Pharmaceutical and Biomedical Sciences, vol. 2, no. 3, pp. 65–80, 2011.

[2] R. Hajiaghaee and S. Akhondzadeh, "Herbal medicine in the treatment of Alzheimer's disease," Journal of Medicinal Plants, vol. 11, no. 41, pp. 1–7, 2012.

[3] S. Akbar, "Andrographis paniculata: a review of pharmacological activities and clinical effects," Alternative Medicine Review, vol. 16, no. 1, pp. 66–77, 2011.

[4] K. Jarukamjorn and N. Nemoto, "Pharmacological aspects of Andrographis paniculata on health and its major diterpenoid constituent andrographolide," Journal of Health Science, vol. 54, no. 4, pp. 370–381, 2008.

[5] R. Ajaya Kumar, K. Sridevi, N. Vijaya Kumar, S. Nanduri, and S. Rajagopal, "Anticancer and immunostimulatory compounds from Andrographis paniculata," Journal of Ethnopharmacology, vol. 92, no. 2-3, pp. 291–295, 2004.

[6] S. Rajagopal, R. A. Kumar, D. S. Deevi, C. Satyanarayana, and R. Rajagopalan, "Andrographolide, a potential cancer therapeutic agent isolated from Andrographis paniculata," Journal of Experimental Therapeutics and Oncology, vol. 3, no. 3, pp. 147–158, 2003.

[7] H.-Y. Cheung, S.-H. Cheung, J. Li et al., "Andrographolide isolated from Andrographis paniculata induces cell cycle arrest and mitochondrial-mediated apoptosis inhuman leukemicHL- 60 cells," Planta Medica, vol. 71, no. 12, pp. 1106–1111, 2005.

[8] W. Li, X. Xu, H. Zhang et al., "Secondary metabolites from Andrographis paniculata," Chemical and Pharmaceutical Bulletin, vol. 55, no. 3, pp. 455–458, 2007.

[9] S. Harjotaruno, A. Widyawaruyantil, andN.C. Zaini, "Apoptosis inducing effect of andrographolide on TD-47 human breast cancer cell line," African Journal of Traditional, Complementary and Alternative Medicines, vol. 4, no. 3, pp. 345–351, 2008.

[10] J. Zhou, S. Zhang, O. Choon-Nam, and H.-M. Shen, "Critical role of pro-apoptotic Bcl-2 family members in andrographolide- induced apoptosis in human cancer cells," Biochemical Pharmacology, vol. 72, no. 2, pp. 132–144, 2006.

[11] Puri, R. Saxena, R. P. Saxena, K. C. Saxena, V. Srivastava, and J. S. Tandon, "Immunostimulant agents from Andrographis paniculata," Journal of Natural Products, vol. 56, no. 7, pp. 995– 999, 1993.

[12] T.Matsuda, M. Kuroyanagi, S. Sugiyama, K. Umehara, A. Ueno, and K. Nishi, "Cell differentiation-inducing diterpenes from Andrographis paniculata Nees," Chemical and Pharmaceutical Bulletin, vol. 42, no. 6, pp. 1216–1225, 1994.

[13] S.Gupta, M. A. Choudhry, J.N. S. Yadava, V. Srivastava, and J. S. Tandon, "Antidiarrhoeal activity of diterpenes of Andrographis paniculata (Kal-Megh) against Escherichia coli enterotoxin in in vivo models," International Journal of Crude Drug Research, vol. 28, no. 4, pp. 273–283, 1990.

[14] W. Tang and G. Eisenbrand, "Andrographis paniculata (Burm. f.) Nees," in Chinese Drugs of Plant Origin Chemistry, Pharmacology, and Use in Raditional and Modern Medicine,

[15] Savita N, Dubey G. Assessment of the antibacterial, antioxidant, and phytochemical potential of Fernandoa adenophylla, Curcuma caesia, and Melaleuca alternifolia. J Chem Health Risks. 2025;15(6):3503–3511.

[16] B.-C. Yu, C.-R.Hung,R\.-C. Chen, and J.-T. Cheng, "Antihyperglycemic effect of andrographolide in streptozotocin-induced diabetic rats," PlantaMedica, vol. 69,no. 12,pp. 1075–1079, 2003.

[17] B. C. Yu, C. K. Chang, C. F. Su, and J. T. Cheng, "Mediation of β-endorphin in andrographolide-induced plasma glucoselowering action in type I diabetes-like animals," Naunyn- Schmiedeberg's Archives of Pharmacology, vol. 377, no. 4–6, pp. 529–540, 2008.

[18] R. Subramanian and M. Z. Asmawi, "Inhibition of α-glucosidase by Andrographis paniculata ethanol extract in rats," Pharmaceutical Biology, vol. 44, no. 8, pp. 600–606, 2006.

[19] R. Subramanian, M. Z. Asmawi, and A. Sadikun, "In vitro α-glucosidase and α-amylase enzyme inhibitory effects of Andrographis paniculata extract and andrographolide," Acta Biochimica Polonica, vol. 55, no. 2, pp. 391–398, 2008.

[20] W. F. Chiou, J. J. Lin, and C. F. Chen, "Andrographolide suppresses the expression of inducible nitric oxide synthase in macrophage and restores the vasoconstriction in rat aorta treated with lipopolysaccharide," British Journal of Pharmacology, vol. 125, no. 2, pp. 327– 334, 1998.

[21] W\.-F. Chiou, C.-F. Chen, and J.-J. Lin, "Mechanisms of suppression of inducible nitric oxide synthase (iNOS) expression in RAW 264.7 cells by andrographolide," British Journal of Pharmacology, vol. 129, no. 8, pp. 1553–1560, 2000.

[22] K. Sheeja, P. K. Shihab, and G. Kuttan, "Antioxidant and anti-inflammatory activities of the plant Andrographis paniculata nees," Immunopharmacology and Immunotoxicology, vol. 28,no. 1, pp. 129–140, 2006.

[23] Y. C. Shen, C. F. Chen, and W. F. Chiou, "Andrographolide prevents oxygen radical production by human neutrophils: possible mechanism(s) involved in its anti-inflammatory effect," British Journal of Pharmacology, vol. 135, no. 2, pp. 399–406, 2002.

[24] Mahajan SS, Savita N, Kumar S. The Important Role of Six Sigma in Pharmaceutical Industry-A Review. Indian Journal of Health Care, Medical & Pharmacy Practice. 2022 Apr.

[25] C.Wiart, K. Kumar, M. Y. Yusof, H. Hamimah, Z.M. Fauzi, and M. Sulaiman, "Antiviral properties of ent-labdene diterpenes The ScientificWorld Journal 21 of Andrographis paniculata Nees, inhibitors of herpes simplex virus type 1," Phytotherapy Research, vol. 19, no. 12, pp. 1069– 1070, 2005.

[26] P.Misra, N. L. Pal, P. Y. Guru, J.C.Katiyar,V. Srivastava, andJ. S. Tandon, "Antimalarial activity of Andrographis paniculata (Kalmegh) against Plasmodium berghei NK 65 in Mastomys natalensis," International Journal of Pharmacognosy, vol. 30, no. 4, pp. 263–274, 1992.

[27] R. E. Kamdem, S. Sang, and C.-T. Ho, "Mechanism of the superoxide scavenging activity of neoandrographolide—a natural product from Andrographis paniculata nees," Journal of Agricultural and Food Chemistry, vol. 50, no. 16, pp. 4662–4665, 2002.

[28] R. P. Singh, S. Banerjee, and A. R. Rao, "Modulatory influence of Andrographis paniculata on mouse hepatic and extrahepatic carcinogen metabolizing enzymes and antioxidant status," Phytotherapy Research, vol. 15, no. 5, pp. 382–390, 2001.

[29] G. A. Akowuah, I. Zhari, and A. Mariam, "Analysis of urinary andrographolides and antioxidant status after oral administration of Andrographis paniculata leaf extract in rats," Food and Chemical Toxicology, vol. 46, no. 12, pp. 3616–3620, 2008.

[30] C. Y. Zhang and B. K. H. Tan, "Mechanisms of cardiovascular activity of Andrographis paniculata in the anaesthetized rat," Journal of Ethnopharmacology, vol. 56, no. 2, pp. 97– 101, 1997.